



Lawrence Berkeley Laboratory

UNIVERSITY OF CALIFORNIA

ENERGY & ENVIRONMENT DIVISION

RECEIVED
LAWRENCE
BERKELEY LABORATORY
FEB 22 1982
LIBRARY AND
DOCUMENTS SECTION

To be presented at the American Society of Heating,
Refrigerating and Air-Conditioning Engineers, Inc.
(ASHRAE) Semi-Annual Meeting, Houston, TX, January
24-28, 1982

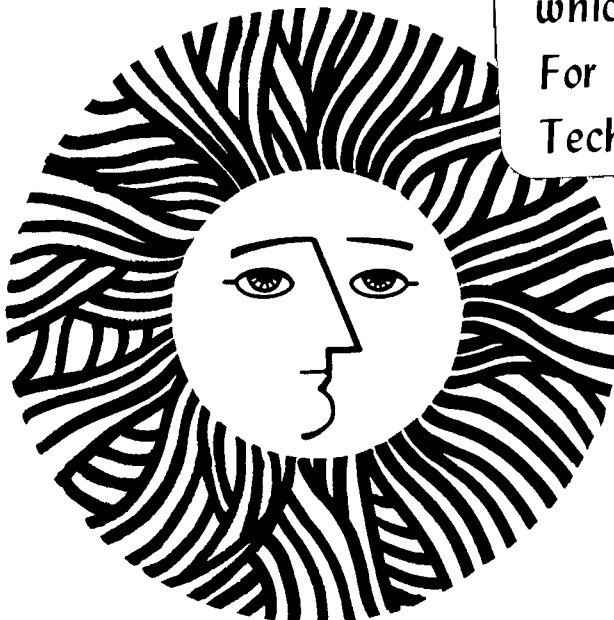
A PREDICTIVE AIR INFILTRATION MODEL--LONG-TERM
FIELD TEST VALIDATION

M.P. Modera, M.H. Sherman, and D.T. Grimsrud

November 1981

TWO-WEEK LOAN COPY

This is a Library Circulating Copy
which may be borrowed for two weeks.
For a personal retention copy, call
Tech. Info. Division, Ext. 6782



LBL-13509
c.2

DISCLAIMER

This document was prepared as an account of work sponsored by the United States Government. While this document is believed to contain correct information, neither the United States Government nor any agency thereof, nor the Regents of the University of California, nor any of their employees, makes any warranty, express or implied, or assumes any legal responsibility for the accuracy, completeness, or usefulness of any information, apparatus, product, or process disclosed, or represents that its use would not infringe privately owned rights. Reference herein to any specific commercial product, process, or service by its trade name, trademark, manufacturer, or otherwise, does not necessarily constitute or imply its endorsement, recommendation, or favoring by the United States Government or any agency thereof, or the Regents of the University of California. The views and opinions of authors expressed herein do not necessarily state or reflect those of the United States Government or any agency thereof or the Regents of the University of California.

Paper to be presented at the American Society of Heating, Refrigerating and Air-Conditioning Engineers, Inc. (ASHRAE) Semi-Annual Meeting, Houston TX, January 24-28, 1982.

A PREDICTIVE AIR INFILTRATION MODEL--LONG-TERM
FIELD TEST VALIDATION

M. P. Modera
M. H. Sherman
D. T. Grimsrud

Energy Performance of Buildings Group
Lawrence Berkeley Laboratory
University of California
Berkeley, CA 94720

NOVEMBER 1981

This work was supported by the Assistant Secretary for Conservation and Renewable Energy, Office of Buildings and Community Systems, Buildings Division of the U.S. Department of Energy under Contract No. W-7405-ENG-48.

ABSTRACT

A predictive model of air infiltration in residential structures is described. This model uses wind speed and outdoor temperature data, along with selected building and site parameters, to predict average infiltration. Long-term field validation results obtained in a portable test structure are presented together with long-term data from three unoccupied test houses at the Owens-Corning Technical Center. The ratio between predicted and measured infiltration peaks near one in all comparisons. The estimated standard deviation of the ratios decreases with longer averaging times. Values decrease from $\pm 35\%$ to $\pm 7\%$ in moving from a 1/2-hour infiltration prediction to a one-week prediction in the portable test structure. In the test houses, the values decrease from $\pm 66\%$ to $\pm 19\%$ in moving from a one-hour prediction of infiltration to a one-week value.

A Predictive Air Infiltration Model - Long-Term
Field Test Validation

M. P. Modera, M. H. Sherman, and D. T. Grimsrud
Energy Performance of Buildings Group
Lawrence Berkeley Laboratory
University of California
Berkeley, CA 94720

INTRODUCTION

Researchers at a national laboratory have developed a model that can be used to predict the air infiltration rate of a residential structure. This model uses wind speed and outdoor temperature data, along with selected building and site parameters, to predict either hour-by-hour or long-term average infiltration.

Until now, the validity of the model has been tested through short-term survey measurements in occupied houses. Although the correlations of predicted and measured infiltration have been good, tests in occupied houses are necessarily restricted in terms of the time spent at any given house and the control of the model parameters for each building and site. This report presents long-term field validation results obtained by means of a portable test structure, the Mobile Infiltration Test Unit. In addition, long-term data from three unoccupied test houses at another research center are used to compare model predictions with measured infiltration data.

INFILTRATION MODEL

The residential infiltration model uses a few building and site parameters to make infiltration predictions from available weather data.^{1,2} The model was specifically designed for simplicity, that is, precise detail was sacrificed for ease of application. The functional form of the model, along with a description of the important assumptions, is presented below.

M. P. Modera, Staff Scientist; M. H. Sherman, Staff Scientist; and D. T. Grimsrud, Staff Scientist, Energy Performance of Buildings Group, Lawrence Berkeley Laboratory, University of California, Berkeley.

The most important factor for determining natural infiltration is the resistance of the building shell to airflow. Air leakage is described in terms of the effective leakage area, which is a measure of the flow area of the cracks and openings in the building shell. Inherent in the definition of effective leakage area is the assumption of square-root flow; i.e., it assumes that the flow through the apertures in the building shell is similar to orifice flow, where the flow rate is proportional to the square root of the pressure drop. This implies that the flow through the building shell can be represented by:

$$Q = L \sqrt{\frac{2}{\rho} \Delta P} \quad (1)$$

where

ΔP is the pressure drop across the building shell (Pa)

L is the effective leakage area (m²)

ρ is the density of air (kg/m³)

This flow model has been verified using measurements of leakage at very low pressures.³

The leakage area is measured with a technique known as fan pressurization, which involves sealing a fan, mounted on an adjustable wooden plate, into the doorway of the house to be tested. The fan speed, which is adjusted using a DC motor and controller, is varied to produce a series of pressure drops, both positive (pressurization) and negative (depressurization) across the building envelope. The flows induced by these pressure differences are determined from the fan calibration. In order to determine the curve relating the pressure drop across the envelope to the flow that it induces, the flows at each pressure differential are plotted on log-log paper. In the pressure region used (+ 10 to + 60 Pa), the data generally form a straight line; i.e., the data are well represented by the empirical relationship:

$$Q = K \Delta P^n \quad (2)$$

where

Q is the volume flow rate of the fan (m³/s)

K is a constant

ΔP is the pressure drop across the building envelope (Pa)

n is an exponent in the range 0.5 < n < 1.0

Since the flow exponent, n, is not always equal to 0.5, the effective leakage area must be evaluated at a particular reference pressure. The pressure selected, 4 Pa, is typical of the weather-induced pressures that cause infiltration. Substituting the reference pressure ($\Delta P_r = 4$ Pa) for ΔP in Eq. 2, then inserting this expression into Eq. 1 and solving for L, yields:

$$L = K \sqrt{\frac{\rho}{2}} (\Delta P_r)^{n - \frac{1}{2}} \quad (3)$$

where

- K is the graphically determined constant
- L is the effective leakage area (m²)
- ρ is the density of air (kg/m³)
- ΔP_r is the reference pressure (Pa)

The basic form of the infiltration model is:

$$Q = L \sqrt{f_s^2 \Delta T + f_w^2 v^2} \quad (4)$$

where

- Q is the infiltration (m³/s)
- L is the effective leakage area (m²)
- ΔT is the indoor-outdoor temperature difference (K)
- f_s is the stack parameter (m/s/K^{1/2})
- v is the wind speed (m/s)
- f_w is the wind parameter

In this expression, f_w and f_s, the wind and stack parameters, essentially convert the wind speed, v, and the indoor-outdoor temperature difference, ΔT, into equivalent pressures across the leakage area of the house. The terms inside the square root actually have the units of velocity squared, i.e., pressure over density. The derivations of these terms are complex, but their interpretation is straightforward.

The wind parameter is given by the following expression:

$$f_w = C' \left[(1 - R)^{1/3} \right] \left[\frac{\alpha \left[\frac{H}{10} \right]^\gamma}{\alpha' \left[\frac{H'}{10} \right]^{\gamma'}} \right] \quad (5)$$

where

- C' is the generalized shielding coefficient
- R is the fraction of leakage on horizontal surfaces
(i.e., the fraction of leakage in the floor and ceiling)
- α, γ are terrain parameters
- H is height of the structure (m)
- H' is the height of the wind measurement (m)

The wind parameter contains three factors: the generalized shielding parameter, the R factor, and the terrain factor. The first factor describes the shielding around the structure; wind tunnel data⁴ have been used to find the generalized shielding coefficient for the case where there are no significant obstructions in the vicinity of the structure, and the concept has been broadened to allow for five different classes of shielding. Shielding class I is the unobstructed case, while the values of the other classes reflect the fact that increasing the amount of obstructions near the structure will lower the pressures acting on that structure. The description of each shielding class and their respective shielding coefficients are displayed in Tab. 1.

Table 1 Generalized Shielding Coefficient (C') for Local Shielding		
Shielding Class	C'	Description
I	0.32	No obstructions (trees, fences, nearby houses) whatsoever
II	0.28	Light local shielding with few obstructions
III	0.24	Some obstructions within two house heights
IV	0.18	Obstructions around most of perimeter
V	0.10	Large obstructions surrounding perimeter within two house heights

This treatment of localized shielding is the portion of the model that contains the greatest uncertainty. The quasi-linear interpretation of shielding presented in Tab. 1 is, at best, an approximation of the complex nonlinear interactions between the building being modeled and nearby obstructions. This point is discussed further below.

The second factor in the wind-parameter expression accounts for the fact that the amount of leakage area exposed to the wind is reduced as the leakage area is shifted from the walls to the floor and ceiling. The model explicitly assumes that the floor and ceiling are shielded from the influence of the wind. R is defined as the ratio of the sum of floor and ceiling leakage areas to the total leakage area of the house:

$$R = \frac{L_{\text{ceiling}} + L_{\text{floor}}}{L} \quad (6)$$

The third factor in the wind-parameter expression accounts for the fact that the wind measured on a weather tower will not be the same as the effective wind speed at the structure. To compensate for this effect, standard wind engineering formulae⁵ are used to translate the wind in one terrain at one height to the same wind in another terrain at another height. The primed quantities in the wind-parameter expression refer to the variables at the wind-measurement site, and the unprimed ones refer to the variables at the structure. Typical values for the terrain parameters are presented in Tab. 2.

Table 2			
Terrain Parameters for Standard Terrain Classes			
Class	γ	d	Description
I	0.10	1.30	Ocean or other body of water with at least 5 km of unrestricted expanse
II	0.15	1.00	Flat terrain with some isolated obstacles (e.g., buildings or trees well separated from each other)
III	0.20	0.85	Rural areas with low buildings, trees, etc.
IV	0.25	0.67	Urban, industrial, or forest areas
V	0.35	0.47	Center of large city

The stack parameter is given by the following expression:

$$f_s = \frac{(1 + R/2)}{3} \left[\frac{\sqrt{8\beta^0} \sqrt{1 - \beta^0}}{\sqrt{\beta^0} + \sqrt{1 - \beta^0}} \right] \sqrt{\frac{gH}{T}} \quad (7)$$

where

- g is the acceleration of gravity (9.8 m/s²)
- H is height of the structure (m)
- T is the inside temperature (295K)
- f_s is the (dimensionless) stack parameter
- β^0 is the (dimensionless) height of the neutral level

The neutral level, β^0 , is the ratio of the height at which the pressure inside exactly equals the pressure outside (due to the stack effect) to the height of the structure. Although this variable is experimentally determinable,⁶ it is impractical to conduct this experiment in the field. A related expression that is more easily estimated is the ratio of the difference between floor and ceiling leakage areas to the total leakage area:

$$X = \frac{L_{\text{ceiling}} - L_{\text{floor}}}{L} \quad (8)$$

The stack parameter can therefore be approximated as:

$$f_s = \frac{(1 + R/2)}{3} \left[1 - \frac{X^2}{(2 - R)^2} \right]^{3/2} \sqrt{\frac{gH}{T}} \quad (9)$$

In principle, R and X could be measured by determining the leakage areas of the floor and ceiling, a cumbersome and time-consuming procedure. Instead, positions of the major leakage sites in the building shell are noted, and the leakage areas of these sites are subtracted from the total value measured for the house. The remaining leakage area is assumed to be distributed uniformly over the shell. A more rigorous measurement procedure is not required, since the model predictions are insensitive to changes in R and X.

A useful physical interpretation of the model is that it converts the complex pressure distributions caused by wind and stack effects into an equivalent single pressure across an aperture with the same effective leakage area as the structure. An immediate corollary of this interpretation is that wind and stack effects are added by simply superimposing the equivalent pressures induced by each effect (Eq. 1). That is, wind-induced infiltration and stack-induced infiltration add in quadrature.

$$Q = \sqrt{Q_{\text{stack}}^2 + Q_{\text{wind}}^2} \quad (10)$$

where

Q is the combined infiltration (m^3/s)

MITU TRAILER

The Mobile Infiltration Test Unit (MITU) is a commercially available construction-site office trailer that was modified and instrumented to permit use for infiltration research. ⁷ Illustrated in Fig. 1, MITU is a portable self-contained test structure designed to perform extended infiltration field studies in a variety of climates, allowing complete control of building parameters and site parameters. It is instrumented to provide for validation of both long-term average and hour-by-hour infiltration-model predictions. The trailer is also designed to test various components of the model individually (i.e., translation of airport wind data into wind at the structure, reduction of wind-induced pressures due to localized shielding, C' , etc.).

MITU is a wood-frame structure, 4.9 m (16 ft) long, 2.4 m (8 ft) wide, and 2.4 m (8 ft) high. It contains both heating and cooling systems and requires only electrical power at each site. The walls and floor of the trailer contain a total of sixteen window openings that can be fitted with interchangeable calibrated leakage panels for controlling total leakage area, leakage distribution, and leakage type (i.e., narrow cracks, large holes). The trailer shell is sealed with a continuous vapor barrier, and perforations are caulked with silicone sealant to minimize the leakage area. The leakage areas of the panels and the trailer shell are determined with a specially designed fan pressurization system that fits into one of the window openings and measures airflow using an orifice plate.

Air infiltration, weather data, and surface pressures are sampled, reduced, and recorded on floppy disk by a Z-80 microprocessor-based computer. Windspeed and wind direction are measured 10 m (33 ft) above the ground using sensors on a weather tower mounted on the trailer.

Air infiltration is monitored with the Continuous Infiltration Monitoring System (CIMS).⁷ This system continuously injects a tracer gas and measures its concentration. The volumetric air infiltration rate is calculated from the equation:

$$C = \frac{F}{Q} + (C_0 - \frac{F}{Q}) e^{-\frac{Qt}{V}} \quad (11)$$

where

- Q is the volumetric air infiltration rate (m³/h)
- F is the tracer gas injection rate (m³/h)
- C is the tracer-gas concentration (ppm)
- C₀ is the tracer-gas concentration at time zero (ppm)
- V is the effective volume of the structure (m³)
- t is the time elapsed since time zero (h)

The CIMS system measures tracer-gas concentration (C), tracer-gas flow rate (F), and elapsed time (t), leaving three unknown parameters: the infiltration rate (Q), the tracer-gas concentration at time zero (C₀), and the effective volume of the structure (V). The unknown parameters are determined by means of a SIMPLEX⁸ likelihood maximization algorithm. The control algorithm then adjusts the tracer-gas flow rate to maintain the concentration within a specified range. Tracer concentration and tracer flow are checked every 30 seconds, and these data are used by the SIMPLEX algorithm every half-hour. The zero drift of the analyzer is checked every 30 minutes, and infiltration rates are stored as half-hour averages.

Surface pressures from 82 taps located on the walls, floor, and ceiling are measured with differential pressure transducers. Taps are opened and closed by solenoid valves controlled by the computer. During sampling, each tap is kept open for 10 seconds. The pressure signal, sampled 40 times per second, is electronically filtered using a one-second time constant in order to eliminate any ringing in the pressure lines due to solenoid operation. The pressures are monitored with pressure transducers on six levels. Four of the transducers are on the walls at 0.23m (0.75 ft), 0.90m (2.95 ft), 1.57m (5.15 ft) and 2.24m (7.35 ft) above the floor of the trailer, while the remaining two transducers are for the ceiling and floor. This system allows for direct measurement of stack-induced pressures and the height of the neutral level. The zero of each transducer is checked every 30 minutes and subtracted from the surface pressures, which are then stored as 30 minute averages.

INFILTRATION MODEL VALIDATION

MITU Field Trip

The Mobile Infiltration Test Unit was stationed in Reno, NV, for the winter of December 1980 to March 1981. The site was chosen for its low temperatures, high winds, and lack of shielding from the wind (Fig. 2). During the four-month period, infiltration and weather data were collected under a variety of conditions; the quantity, shape, and distribution of the leakage area were varied, as well as the orientation of the trailer on the site. Half-hour average infiltration predictions were made for 34 days using weather data and appropriate values for each of the model parameters.

A compact method of displaying this type of data is with a histogram of the ratios of predicted-to-measured infiltration. Fig. 3(a) shows the distribution of this ratio for half-hour average infiltration rates; it can be represented by a log-normal distribution having a geometric mean ratio of 1.17. The deviation of the (geometric) mean ratio from unity represents the expected systematic error in model predictions, while the width of the curve is an estimate of the variation of an individual value about the mean. The spread factor, 1.34 in this case, is analogous to the standard deviation of a normal (Gaussian) distribution; the natural log of the spread factor is the standard deviation of the natural log of the ratios. The range corresponding to one standard deviation is determined by multiplying and dividing by the spread factor.

Fig. 3(b) and 3(c) use the same data points as Fig. 3(a), the distinction being that they use 48-data-point (one-day) and 336-data-point (one-week) averages to calculate the ratios. For these longer averaging intervals, one may observe that both the mean ratio and the spread factor move closer to unity. Since overprediction and underprediction errors tend to cancel each other upon averaging, the spread factor is expected to decrease as the averaging time increases.

Although the histograms display systematic errors, they do not provide any information about the tracking ability of the model. Fig. 4 is a plot of air infiltration rate vs time for a three-day period, and Fig. 5 displays the results of a four-day test in another trailer configuration. Measured infiltration is plotted as a solid line, and predicted infiltration is represented by the dotted line. In both figures, the model predictions track measured infiltration quite well, even when the infiltration rate changes by a factor of 10 over the course of the four-day test. These results encourage using the model to provide short-term infiltration predictions in situations that require hour-by-hour infiltration measurements, e.g., measurement of the thermal characteristics of buildings, indoor air quality tests, etc.

The long-term average infiltration rate is an important value for both annual energy use and indoor air quality, since the effects of certain contaminants (such as radon gas) are dependent upon long-term exposure. In many instances, the detailed weather information needed to determine hourly infiltration rates is not available, and the long-term infiltration must be determined using averaged weather. When long-term weather averages are used to approximate the average infiltration rate of the MITU facility during the 34-day period, the predicted average

infiltration rate is 32.9 m³/h. The average infiltration rate measured during this time period was 32.5 m³/h, while the average of the infiltration predictions from half-hour weather readings was 34.4 m³/h.

Although the success of the model predictions is encouraging, it is not surprising that a structure as simple as MITU can be modelled. A more definitive test of a model is to measure its ability to predict infiltration in a real house.

Test Houses

Over the course of a one-year period, researchers at a technical center in Granville, OH, measured the air infiltration rates of three unoccupied test houses. The houses were of standard design and were identical except for insulation levels. They were built to examine the effect of different insulation strategies on heating and cooling loads. From the point of view of infiltration, an important distinction of one house (House C) is the presence of a larger furnace and duct system to compensate for its lack of insulation.

The infiltration rates of the houses were continuously monitored with an injection-decay tracer gas technique, and wind speed and outdoor temperature were monitored with an on-site weather station. This data set, comprised of hourly averages, is one of the most complete descriptions of the infiltration performance of single-family housing in the United States. The on-site weather, was used, along with site descriptions and the results of fan pressurization tests, to make hourly infiltration rate predictions. Tab. 3 summarizes the values of the model parameters used for each house.

Table 3 Model Parameters for Test Houses					
House	Leakage Area L(cm ²)	Leakage Distribution R	Neutral Level β ^o	Shielding Class	Terrain Class
A	470	0.65	0.4	II	II
B	439	0.65	0.4	II	II
C	648	0.65	0.4	II	II

As was done for the MITU trailer, the data for each house are presented in three histograms of predicted/measured ratios (Figs. 6, 7, and 8). In all three houses, although the mean ratios are within 15% of unity, the widths and shapes of the distributions are not as good as those for the MITU trailer. The spread factors for the nine histograms summarized in Tab. 4 should be compared to MITU's hourly, daily, and weekly spread factors of 1.34, 1.17, and 1.07.

House	1 hour Average	1 day Average	1 week Average
A	1.57	1.27	1.18
B	1.62	1.28	1.23
C	1.78	1.46	1.17

In addition to the large spread factors, the distributions for all three houses do not appear to be log-normal. House A is the best of the three, houses B and C having apparently random spikes. Although longer averaging intervals tend to narrow the distributions, they do not seem to provide any significant improvement to the shapes (symmetry) of the distributions.

Before attempting to explain these discrepancies, the added uncertainties involved in using data that are collected by others should be noted. All measured infiltration values in the data sample supplied by the Ohio researchers have been included. In examining the data, a puzzling periodicity in the measurements was noticed. An example is Fig. 9, a plot of measured and predicted infiltration for a short section of data from House C. The measured infiltration rate appears to oscillate at a set frequency of approximately one cycle every eight hours. The Ohio researchers had also seen these effects and explained that it was related to the periodic injection of tracer gas into the houses. Immediately after injection, flow of tracer from conditioned to unconditioned spaces causes a high initial value for the measured infiltration; return flow of the tracer from unconditioned to conditioned spaces causes a measurement error of the opposite sign. These measurement problems will tend to increase the widths of the distributions (Fig. 6,7,8). This particular measurement artifact is more likely to occur when making infiltration measurements using tracer gas decays than when one uses controlled flow or constant concentration techniques.

A significant problem for this model - and for all models that do not use direct measurements of exterior pressures - is the uncertainty of the localized shielding of the structure. It is estimated that the uncertainty in this term (which directly affects the ability to predict wind-driven infiltration) is approximately 25%. This is an inherent limitation in the ability of this infiltration model to make short-term infiltration predictions based upon leakage area measurements.

Despite the difficulties described above, if one attempts to predict the long-term average infiltration rates of these structures using averaged weather data, the results are surprisingly good. Tab. 5 compares measured average infiltration, average predicted infiltration, and predicted average infiltration (using averaged weather). As in the case of the MITU trailer, the use of averaged weather data gives reasonably accurate predictions of long-term average infiltration. The deviation of the predicted average from the measured value is 16% at most--a degree of accuracy equivalent to that obtained by averaging hourly infiltration predictions.

Table 5 Average Infiltration in Test Houses (m ³ /h) ^a			
House	Average Measured	Average Predicted	Predicted Average
A	74.4	66.9	68.1
B	72.9	75.7	80.3
C	87.4	99.4	101.1
^a House volume is 314 m ³ in each case			

CONCLUSIONS

Having compared model predictions with measured infiltration rates in the MITU trailer, one may conclude that the model can be used to predict both long-term and hour-by-hour infiltration rates. For the entire 34-day data set, the half-hour infiltration predictions have an accuracy of 35%, the daily infiltration predictions are within 20%, and the weekly infiltration predictions are within 10%. The comparison of model predictions with the infiltration rates measured in three test houses was not as conclusive. Although the long-term average infiltration rates were within 20% of the measured values, the tracking ability of the model could not be verified by means of the existing data.

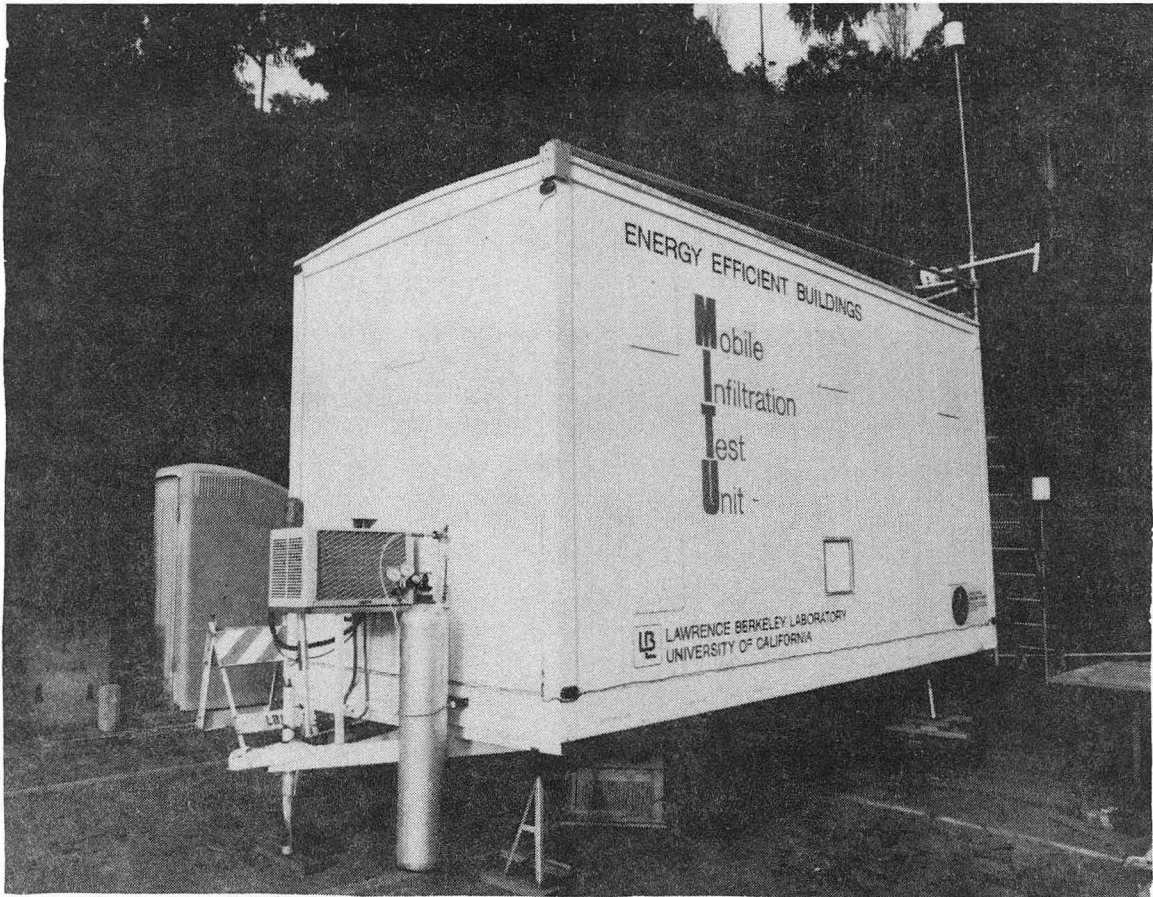
Additional reduction of MITU data is presently in progress. An important part of this work is the determination of the generalized shielding coefficient from surface pressure measurements. This important parameter needs to be measured at a variety of test sites in order to facilitate site classification. The MITU trailer is also well suited for comparing airport weather station data with the actual wind speeds at the test site. These tests also require using a variety of test sites within varying distances of the airport weather station. concerning the Owens Corning infiltration measurements.

REFERENCES

1. Sherman, M.H., "Air Infiltration in Buildings," Lawrence Berkeley Laboratory report, LBL-10712, 1981.
2. Sherman, M.H., and Grimsrud, D.T., "The Measurement of Infiltration Using Fan Pressurization and Weather Data," in Proceedings of the First International Air Infiltration Centre Conference, London 1980, Lawrence Berkeley Laboratory report, LBL-10852, 1981.
3. Sherman, M.H., Grimsrud, D.T., and Sonderegger, R.C., "The Low Pressure Leakage Function of a Building," Proceedings of the ASHRAE/DOE-ORNL Conference "Thermal Performance of the Exterior Envelopes of Buildings," December 3-5, 1979, ASHRAE, New York, 1981.
4. Akins, R.E., Peterka, J.A., and Cermak, J.E., "Average Pressure Coefficients for Rectangular Buildings," Proceedings of the Fifth International Conference Wind Engineering, Boulder, CO, July 1979.
5. European Convention for Constructional Steelwork, "Recommendations for the Calculation of Wind Effects on Buildings and Structures," Technical General Secretariat, Brussels, Belgium, Sept. 1978.
6. Sherman, M.H., Grimsrud, D.T., and Diamond, R.C., "Infiltration-Pressurization Correlation: Surface Pressures and Terrain Effects," ASHRAE Transaction 85, 2:458-479, 1979; Lawrence Berkeley Laboratory report, LBL-8785 (1979).
7. Blomsterberg, A.K., Modera, M.P., and Grimsrud, D.T., "The Mobile Infiltration Test Unit--Its Design and Capabilities: Preliminary Experimental Results," Lawrence Berkeley Laboratory report, LBL-12259, 1981.
8. Nelder and Mead, Computer Journal, 7, 308, 1967.

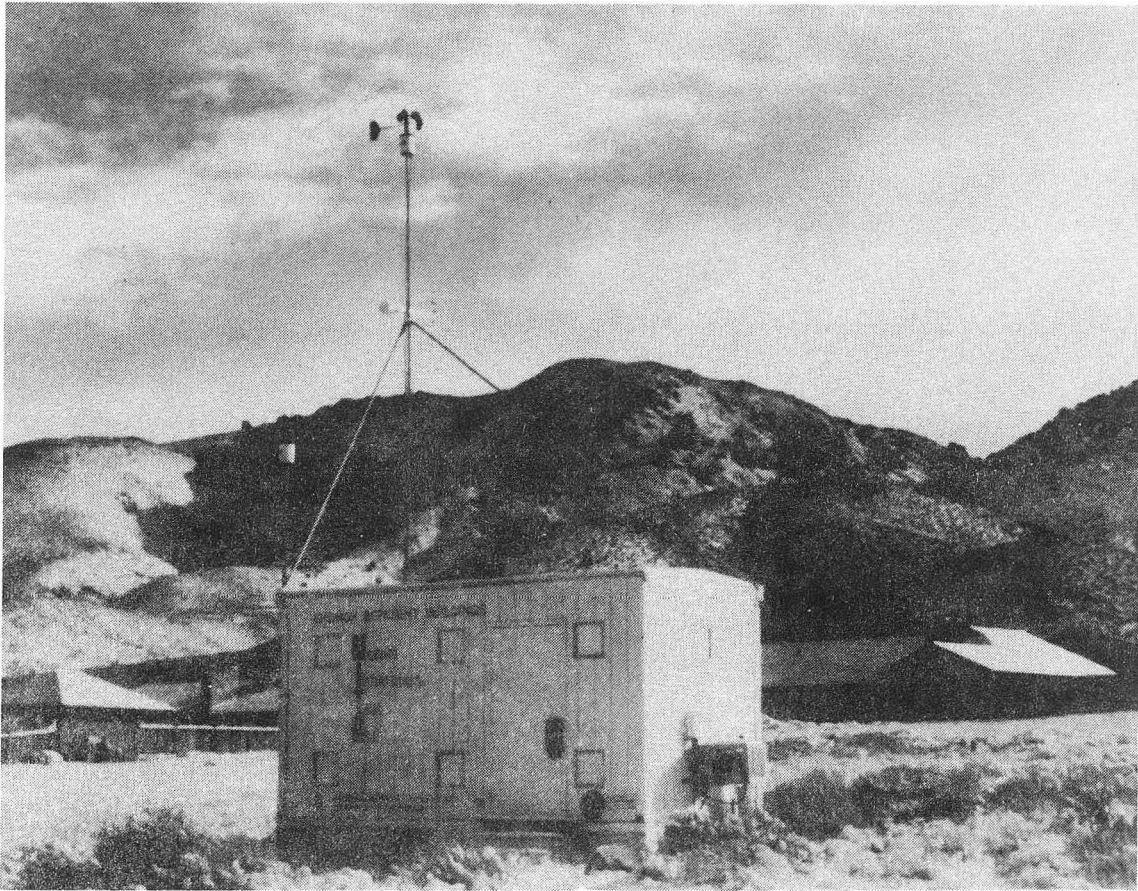
ACKNOWLEDGMENTS

This work was funded by the Assistant Secretary for Conservation and Renewable Resources, Office of Buildings and Community Systems, Buildings Divisions U.S. Department of Energy, under contract No. W-7405-Eng-48. The authors are indebted to Darryl Dickerhoff, Research Technician, and Brian Smith, Computer Scientist, for assistance in obtaining and analyzing the data from MITU. Our special thanks are also extended to Michael Stewart of the Owens Corning Technical Center for discussions



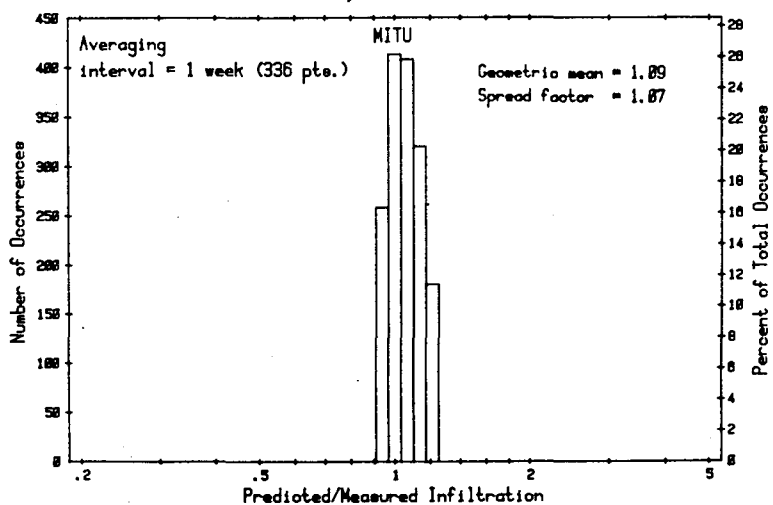
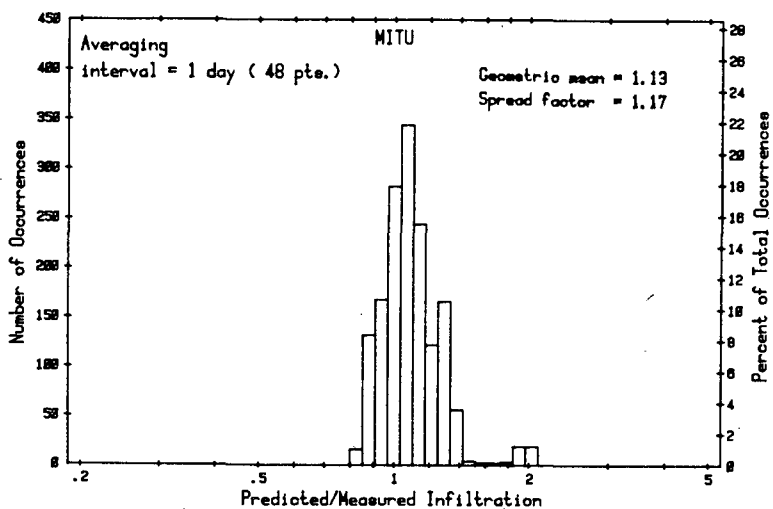
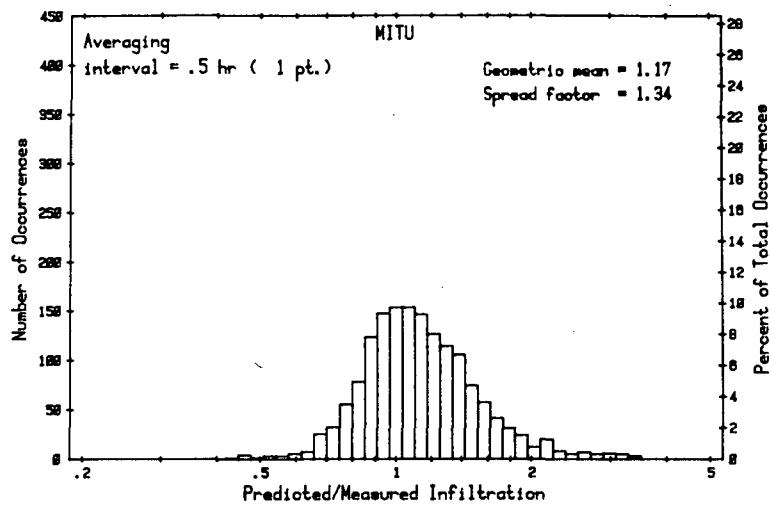
CBB 800-13932

Figure 1. Exterior view of Mobile Infiltration Test Unit in Blackberry Canyon at Lawrence Berkeley Laboratory.



CBB 814-3957

Figure 2. MITU trailer at test site (Reno, Nevada).



XBL 819-1984B

Figure 3. Histograms of MITU data at three different averaging levels.

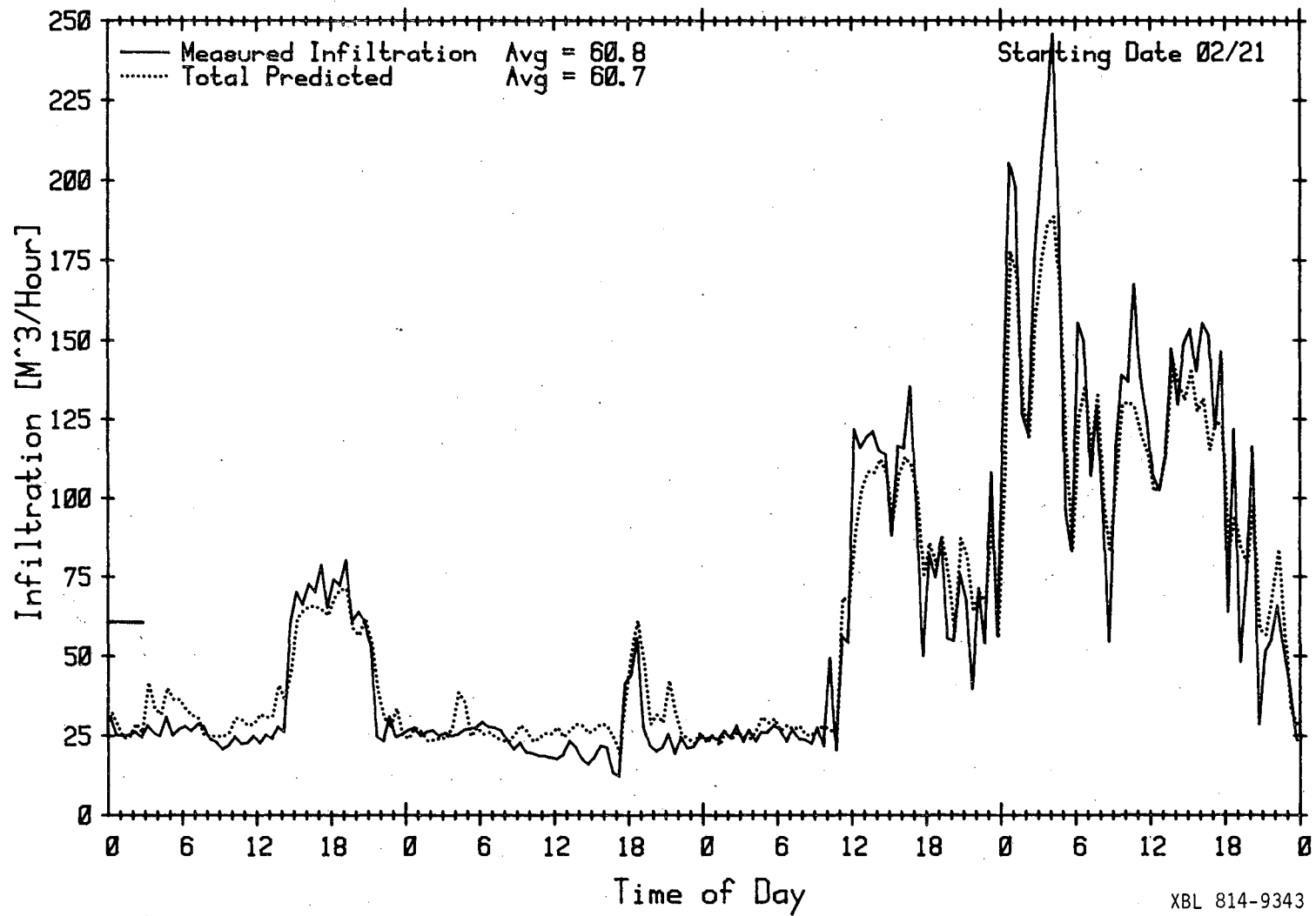
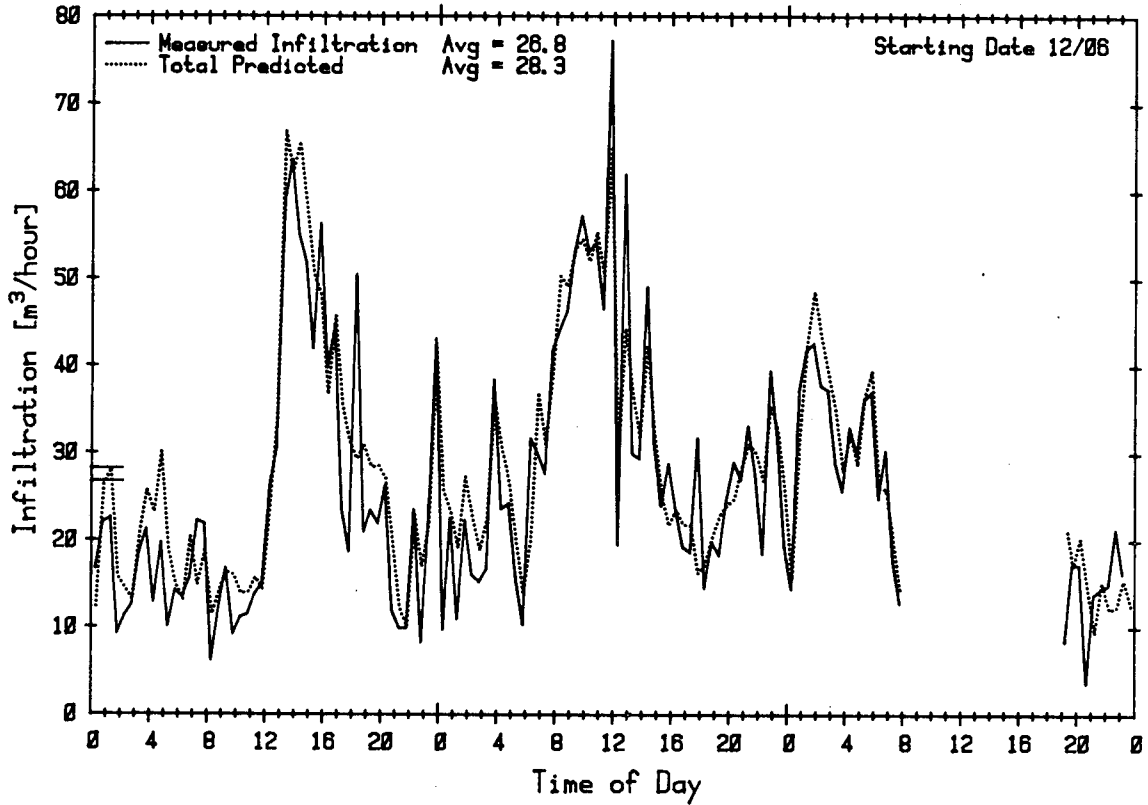
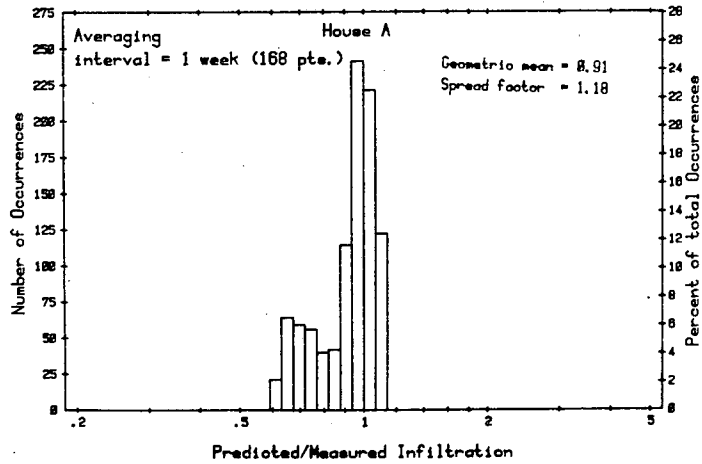
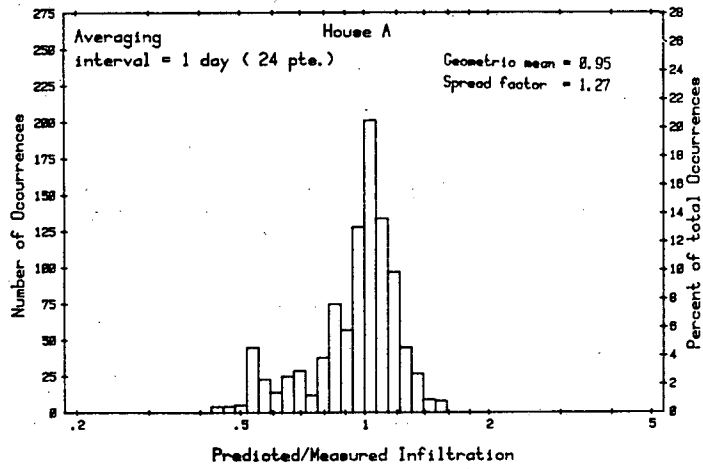
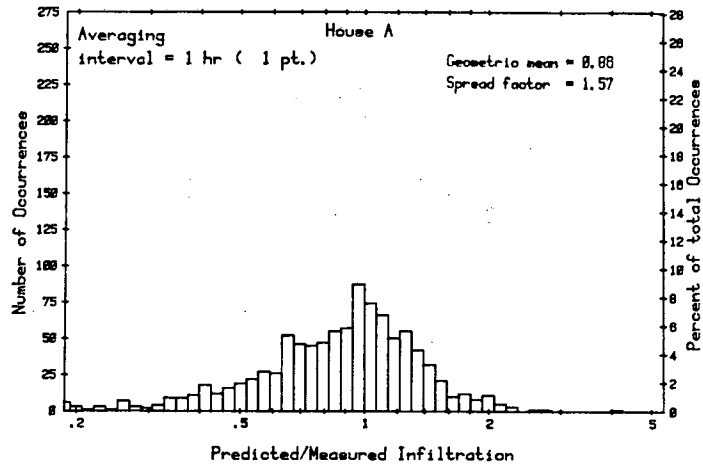


Figure 4. Plot of measured and predicted infiltration vs. time: three-day test in MITU.



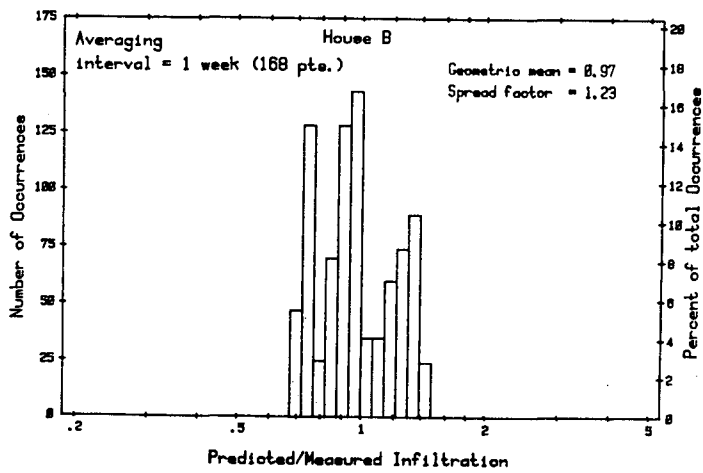
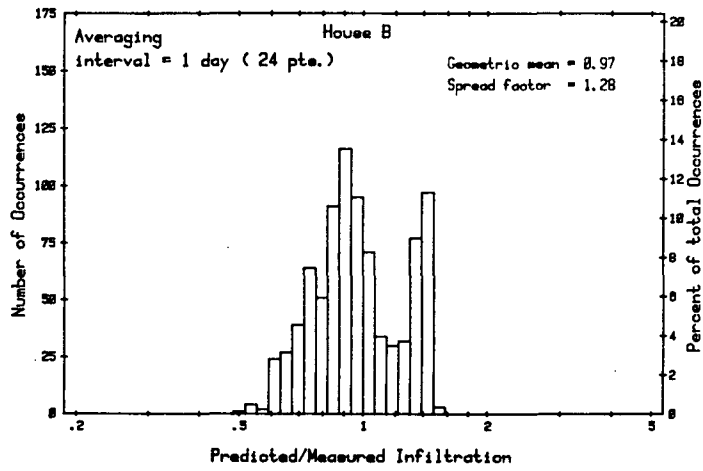
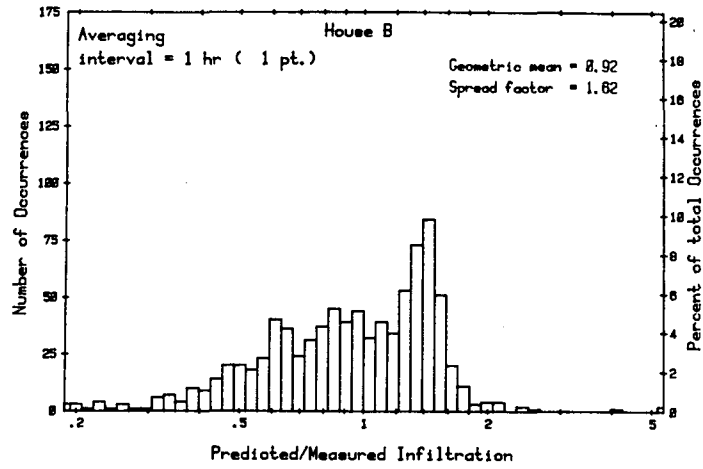
XBL 818-11004

Figure 5. Plot of measured and predicted infiltration vs. time: four-day test in MITU.



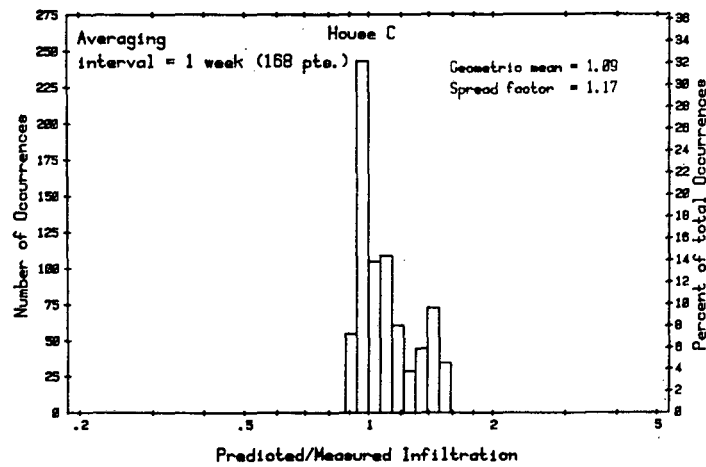
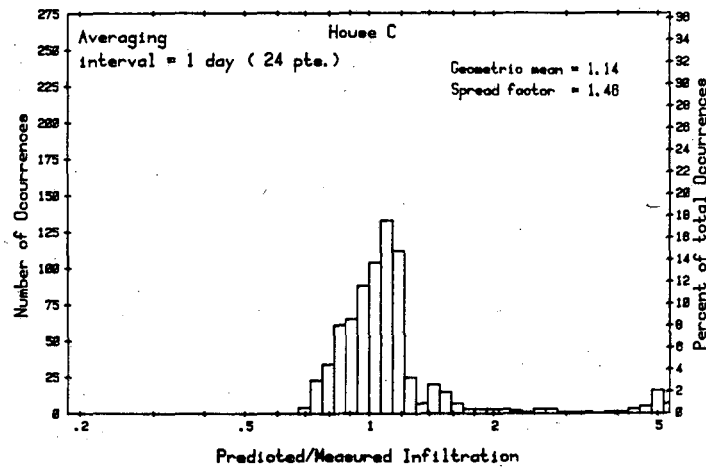
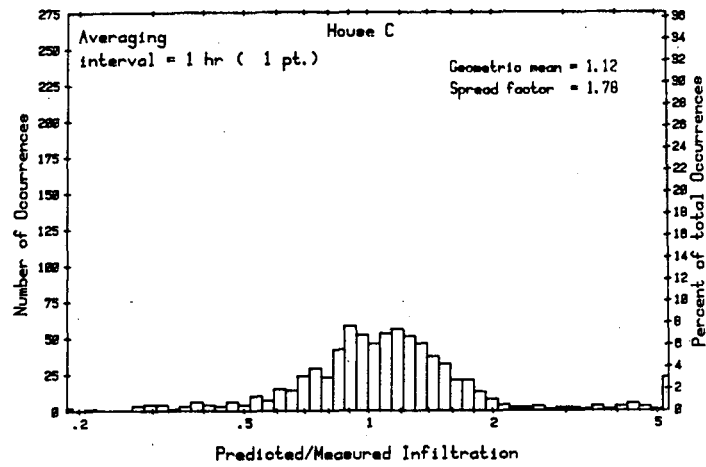
XBL 8111-12463

Figure 6. Histograms of three different averaging intervals for Owens Corning test house A.



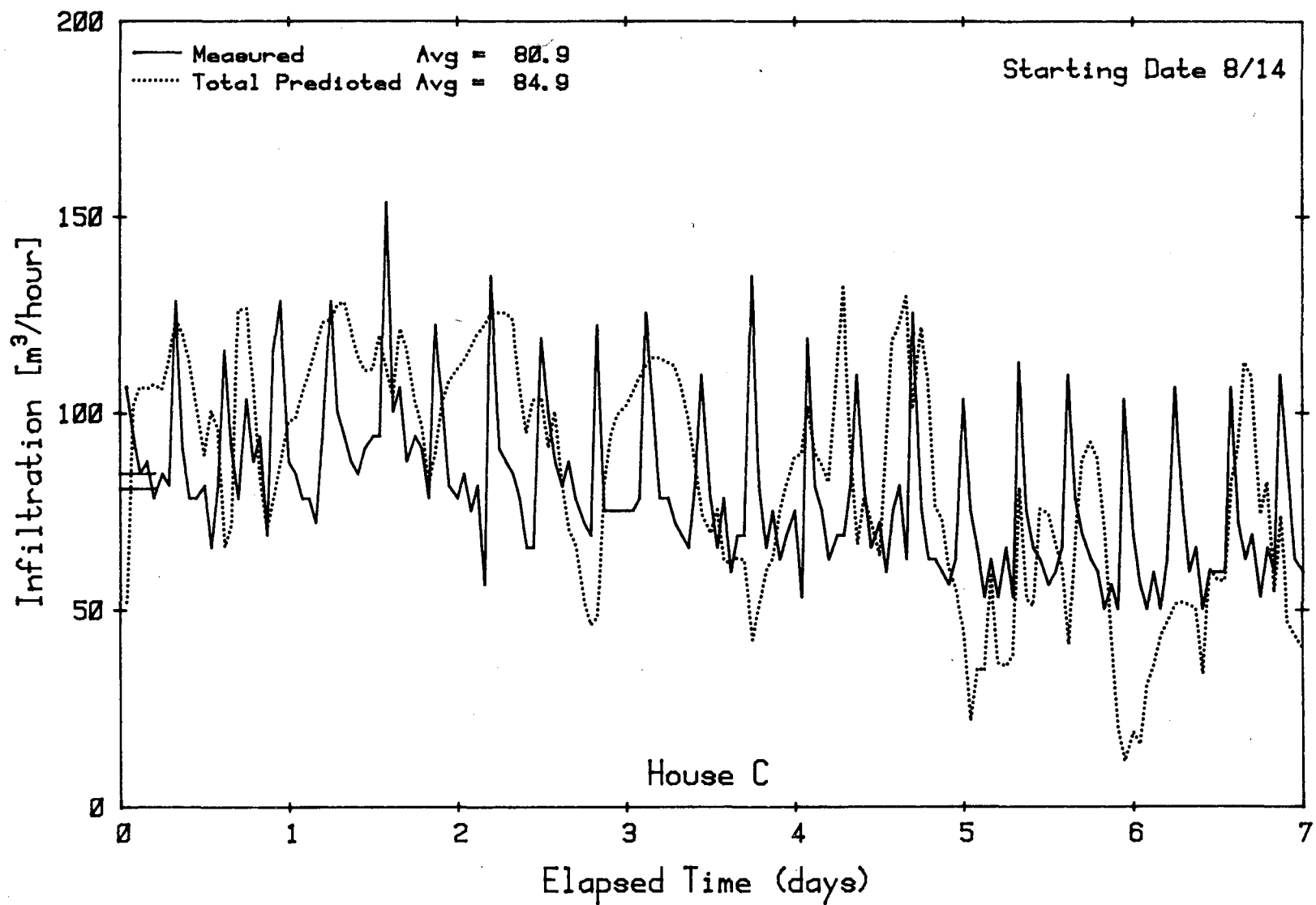
XBL 8111-12464

Figure 7. Histograms at three different averaging intervals for Owens Corning test house B.



XBL 8111-12465

Figure 8. Histograms at three different averaging intervals for Owens Corning test house C.



XBL 8111-12462

Figure 9. Plot of measured and predicted infiltration vs. time: seven-day test in house C.

This report was done with support from the Department of Energy. Any conclusions or opinions expressed in this report represent solely those of the author(s) and not necessarily those of The Regents of the University of California, the Lawrence Berkeley Laboratory or the Department of Energy.

Reference to a company or product name does not imply approval or recommendation of the product by the University of California or the U.S. Department of Energy to the exclusion of others that may be suitable.

TECHNICAL INFORMATION DEPARTMENT
LAWRENCE BERKELEY LABORATORY
UNIVERSITY OF CALIFORNIA
BERKELEY, CALIFORNIA 94720